

Rényi entanglement asymmetry in 1+1-dimensional conformal field theories

Miao Chen^{a*}, Hui-Huang Chen^{a†}

December 19, 2023

^a*College of Physics and Communication Electronics, Jiangxi Normal University,
Nanchang 330022, China*

Abstract

In this paper, we consider the Rényi entanglement asymmetry of excited states in the 1+1 dimensional free compact boson conformal field theory (CFT) at equilibrium. We obtain a universal CFT expression written by correlation functions for the charged moments via the replica trick. We provide detailed analytic computations of the second Rényi entanglement asymmetry in the free compact boson CFT for excited states $\Psi = V_\beta + V_{-\beta}$ and $\Phi = V_\beta + J$ with V_β and $J = i\partial\phi$ being the vertex operator and current operator respectively. We make numerical tests of the universal CFT computations using the XX spin chain model. Taking the non-Hermitian fake RDMs into consideration, we propose an effective way to test them numerically, which can be applied to other excited states. The CFT predictions are in perfect agreement with the exact numerical calculations.

arXiv:2310.15480v2 [hep-th] 16 Dec 2023

*miaoichen1208@163.com

†chenhh@jxnu.edu.cn

Contents

1	Introduction	1
2	Entanglement asymmetry	2
3	Entanglement asymmetry in CFT	4
3.1	Entanglement of excited states in CFT	4
3.2	Entanglement asymmetry in CFT	5
4	Excited states in the free compact boson CFT	6
4.1	Excited state I : $ \Psi\rangle = V_\beta\rangle + V_{-\beta}\rangle$	7
4.2	Excited state II : $ \Phi\rangle = V_\beta\rangle + J\rangle$	8
5	Numerical tests	8
5.1	Excited state I : $ \Psi\rangle = V_\beta\rangle + V_{-\beta}\rangle$	10
5.2	Excited state II : $ \Phi\rangle = V_\beta\rangle + J\rangle$	11
6	Conclusion	12
A	Correlation functions of vertex operators	13
B	Correlation functions of vertex and derivative operators	13
C	RDMs and Correlation matrices in the XX spin chain	14
D	Non-Hermite fake RDMs and Correlation matrices	16

1 Introduction

In recent years, there has been a strong research interest in the interplay between the entanglement and symmetries. In condensed matter physics, entanglement is a powerful tool to characterize different phases of matter. In the studies of thermalizations of isolated quantum systems, people found that entanglement is a crucial quantity that characterizes how the subsystem reach equilibrium. [1–4]. As the most important concept in modern physics, symmetry and its breaking of a quantum system can lead to a large number of interesting phenomena like ferromagnetism [5], superfluidity [6] and superconduction. There exist a vast number of references discussing how entanglement decompose under global symmetries both in and out of equilibrium. See for example [7–22] and references therein. Recently, these theoretical studies have also been confirmed experimentally [23–26].

Entanglement entropy or Von Neumann entropy is the most useful entanglement measure to characterize the bipartite entanglement of a pure state. If we prepare our system in a pure state $|\psi\rangle$, the reduced density matrix (RDM) of the subsystem A is obtained by tracing out degrees of freedom that are not in A , i.e. $\rho_A = \text{tr}_{\bar{A}} |\psi\rangle \langle \psi|$, where \bar{A} is the complement of A . One can compute the von Neumann entropy from $\text{Tr} \rho_A^n$ via the replica trick [1]

$$S_A \equiv -\text{Tr}(\rho_A \log \rho_A) = \lim_{n \rightarrow 1} S_A^{(n)}, \quad (1.1)$$

where $S_A^{(n)}$ is the Rényi entropies

$$S_A^{(n)} = \frac{1}{1-n} \log \text{Tr} \rho_A^n. \quad (1.2)$$

Recently, the concept of entanglement asymmetry is proposed in [27] as a tool to measure the degree of symmetry breaking in extended quantum systems. Universal formula for matrix product states with finite bond dimension has been obtained in [28]. In quantum quench problems, the entanglement asymmetry plays a crucial role in exploring whether the initially broken symmetry can be restored at late times [27, 29–32]. Moreover, it helps in finding a kind of quantum Mpemba effect [27, 33] and leads to new forms of weak and strong Mpemba effects [34]. Very recently, the microscopic origin of the quantum Mpemba effect in integrable systems has been discussed in [33].

However, most of the references mentioned above are focused on the time evolution of entanglement asymmetry. As a new and very important quantity, it is valuable to investigate the properties even at equilibrium. In this paper, we are interested in the calculations of entanglement asymmetry of excited states in CFT at equilibrium. To construct states which have non-vanish entanglement asymmetry, we need to consider the superposition states and non-Hermitian terms will occur in the corresponding RDMs. To numerically test our analytical predictions, special attention need to paid to these non-Hermitian terms. Similar quantities also appear in other field of research, see for example [35–37].

The remaining part of this paper is organized as follows. In section 2, we briefly review the concept of entanglement asymmetry and related quantities. In section 3, we discuss how to compute the entanglement asymmetry in conformal field theories (CFT). In section 4, we focus on a particular CFT i.e. the free compact boson theory and make explicit calculations of the Rényi entanglement asymmetry for two types of excited states with Rényi index $n = 2$. In section 5, we numerically test our field theory predictions in the XX spin chain. Finally, we conclude in section 6 and all technical details are presented in four appendices.

2 Entanglement asymmetry

We prepare an extended quantum system in a pure state $|\psi\rangle$, and divide the system into two spatial regions A and B . The reduced density matrix (RDM) $\rho_A = \text{Tr}_B |\psi\rangle \langle \psi|$ describes the state of the subsystem A . We consider a charge operator $Q = Q_A + Q_B$ which is the generator of a global $U(1)$ symmetry group. We assume that the state $|\psi\rangle$ is not an eigenstate of Q , then $[\rho_A, Q_A] \neq 0$. Therefore, ρ_A displays off-diagonal elements in the eigenbasis of the subsystem charge Q_A .

For later's convenience, we introduce the quantity $\rho_{A,Q}$ which can be obtained by removing the off-diagonal elements of ρ_A ,

$$\rho_{A,Q} = \sum_{q \in \mathbb{Z}} \Pi_q \rho_A \Pi_q, \quad (2.1)$$

where Π_q is the projector onto the eigenspace of Q_A with charge q . Clearly, $\rho_{A,Q}$ is a block diagonal matrix, i.e. $[\rho_{A,Q}, Q_A] = 0$. In Fig. 1, we show the form of ρ_A and $\rho_{A,Q}$ intuitively.

To measure the extent to which the symmetry generated by Q is broken in the subsystem A , the entanglement asymmetry is introduced in [27] and defined as

$$\Delta S_A = S(\rho_{A,Q}) - S(\rho_A). \quad (2.2)$$

It can quantify the symmetry breaking at the level of subsystem A . Obviously, the entanglement asymmetry is only zero when ρ_A commutes with Q_A i.e. $[\rho_A, Q_A] = 0$, and it is always non-negative, $\Delta S_A \geq 0$ [38].

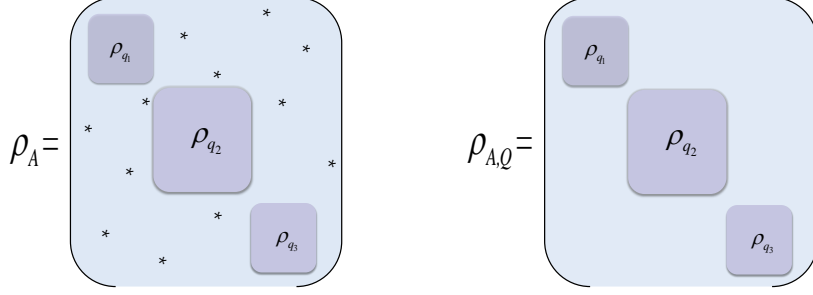


Figure 1: The schematic comparison of the structure of the density matrices ρ_A and $\rho_{A,Q}$ in the eigenbasis of the subsystem charge Q_A . The RDM ρ_A contains non-diagonal elements. Instead, $\rho_{A,Q}$ obtained under a projective measurement of Q_A , is a block diagonal matrix. The entanglement asymmetry is given by the difference $\Delta S_A^{(n)}$ between the entanglement entropies.

Using the same strategy to get the Von Neumann entropy, we can define the Rényi entanglement asymmetry as

$$\Delta S_A^{(n)} = S^{(n)}(\rho_{A,Q}) - S^{(n)}(\rho_A) = \frac{1}{1-n} [\log \text{Tr}(\rho_{A,Q}^n) - \log \text{Tr}(\rho_A^n)]. \quad (2.3)$$

Then ΔS_A can be accessed from $\Delta S_A^{(n)}$ by taking the limit $n \rightarrow 1$,

$$\Delta S_A = \lim_{n \rightarrow 1} \Delta S_A^{(n)}. \quad (2.4)$$

The Rényi entanglement asymmetry are also non-negative, $\Delta S_A^{(n)} \geq 0$, and they vanish only if $[\rho_A, Q_A] = 0$ [39]. Now consider the system with conserved charge $Q = Q_A + Q_B$, with $[\rho_A, Q_A] \neq 0$. The density matrix $\rho_{A,Q}$ can be written as block diagonal forms, $\rho_{A,Q} = \sum_{q \in \mathbb{Z}} \Pi_q \rho_A \Pi_q$. Using the integral representation of Π_q

$$\Pi_q = \int_{-\pi}^{\pi} \frac{d\alpha}{2\pi} e^{i\alpha Q_A} e^{-i\alpha q}, \quad (2.5)$$

we can obtain the post-measurement density matrix $\rho_{A,Q}$ [27] as

$$\rho_{A,Q} = \int_{-\pi}^{\pi} \frac{d\alpha}{2\pi} e^{-i\alpha Q_A} \rho_A e^{i\alpha Q_A}. \quad (2.6)$$

Then we can write the moments of $\rho_{A,Q}$ as

$$\text{Tr}(\rho_{A,Q}^n) = \int_{-\pi}^{\pi} \frac{d\alpha_1 \dots d\alpha_n}{(2\pi)^n} Z_n(\boldsymbol{\alpha}), \quad (2.7)$$

where $\boldsymbol{\alpha} = \{\alpha_1, \dots, \alpha_n\}$ and

$$Z_n(\boldsymbol{\alpha}) = \text{Tr} \left[\prod_{j=1}^n \rho_A e^{i\alpha_{j,j+1} Q_A} \right], \quad (2.8)$$

with $\alpha_{ij} \equiv \alpha_i - \alpha_j$ and $\alpha_{n+1} = \alpha_1$. $\text{Tr}(\rho_{A,Q}^n)$ are the Fourier transform of the partition function on the n -sheet Riemann surface. We can find that if $[\rho_A, Q_A] = 0$, $Z_n(\boldsymbol{\alpha}) = Z_n(0)$, thus $\text{Tr}(\rho_{A,Q}^n) = \text{Tr}(\rho_A^n)$ and $\Delta S_A^{(n)} = 0$. Similar to the case of symmetry resolved entanglement, we call $Z_n(\boldsymbol{\alpha})$ as *charged moments* [7].

The ratio of $\text{Tr}(\rho_{A,Q}^n)$ and $\text{Tr}(\rho_A^n)$ is direct related to the Rényi entanglement asymmetry. For further calculation, it's convenient to define

$$g_n(A) = \frac{\text{Tr}(\rho_{A,Q}^n)}{\text{Tr}(\rho_A^n)}. \quad (2.9)$$

As a result, according to eq. (2.3), the Rényi entanglement asymmetry $\Delta S_A^{(n)}$ can be given by $g_n(A)$,

$$\Delta S_A^{(n)} = \frac{1}{1-n} \log g_n(A). \quad (2.10)$$

In terms of eq. (2.7), the Fourier transform of the ratio $g_n(A)$ is

$$g_n(\boldsymbol{\alpha}, A) = \frac{\text{Tr}(\prod_{j=1}^n \rho_A e^{i\alpha_{j,j+1} Q_A})}{\text{Tr}(\rho_A^n)}, \quad (2.11)$$

which will be used in the latter section.

From the analysis in this subsection, to compute the Rényi entanglement asymmetry, the most important step is calculating $g_n(\boldsymbol{\alpha}, A)$. In next two sections, we will discuss how to compute it in a special CFT, i.e. the free compact boson CFT.

3 Entanglement asymmetry in CFT

3.1 Entanglement of excited states in CFT

In this section, let's review the replica trick to the entanglement asymmetry in 1+1 dimensional CFT. We consider a periodic 1D system with one spatial dimension, total length L , and subsystem A given by the interval $[u, v]$ with length $l = v - u$. It's useful to introduce the dimensionless parameter $x = \frac{v-u}{L} = \frac{l}{L}$, which characterize the size of the subsystem A .

An infinite cylinder with circumference L can be described as the world sheet of the 1+1 dimensional CFT and parameterized by the introduction of complex coordinate z . We are interested in the excited states corresponding to local primary operators

$$|\Upsilon\rangle = \Upsilon(-i\infty) |0\rangle, \quad (3.1)$$

where $|0\rangle$ is the CFT ground state. In the previous section, we have defined the reduced density matrix (RDM) of subsystem A as $\rho_\Upsilon = \text{Tr}_B |\Upsilon\rangle \langle \Upsilon|$. Here we have omit the subscript A and stress on the operator which creates the state. The reduced density matrix of the ground state which corresponds to the identity operator I is written as ρ_I . It's convenient to define the ratio

$$G_n^\Upsilon(x) \equiv \frac{\text{Tr}(\rho_\Upsilon^n)}{\text{Tr}(\rho_I^n)}. \quad (3.2)$$

Following the usual strategy, we can obtain $\text{Tr}(\rho_I^n)$ if we sew cyclically n copies of the above cylinders along with the interval $[u, v]$. Different from the ground state case, there are two additional insertions of $\Upsilon(-i\infty)$ and $\Upsilon^\dagger(i\infty)$ in the corresponding path-integral representation of the reduced density matrix ρ_Υ . In this way, end up with a n -sheeted Riemann surface \mathcal{R}_n . Arriving at a $2n$ -point function, $G_n^\Upsilon(x)$ is straightforwardly given [40–42]

$$G_n^\Upsilon(x) = \frac{\left\langle \prod_{j=1}^n \Upsilon(z_j^-) \Upsilon^\dagger(z_j^+) \right\rangle_{\mathcal{R}_n}}{\langle \Upsilon(z_1^-) \Upsilon^\dagger(z_1^+) \rangle_{\mathcal{R}_1}^n}, \quad (3.3)$$

where z_j^\mp is points inserting the operators in the j -th copy of the system ($j = 1, \dots, n$) in \mathcal{R}_n . Obviously, \mathcal{R}_1 is just the cylinder and $G_1^\Upsilon(x) = 1$, for the normalisation of the involved matrices.

Apply the conformal mapping

$$w(z) = -i \log \left(-\frac{\sin \frac{\pi(z-u)}{L}}{\sin \frac{\pi(z-v)}{L}} \right)^{1/n}, \quad (3.4)$$

to transform the n -sheet Riemann surface \mathcal{R}_n into a single cylinder. The transformation law of a primary field \mathcal{O} is

$$\mathcal{O}(w, \bar{w}) = \left(\frac{dz}{dw} \right)^{h_{\mathcal{O}}} \left(\frac{d\bar{z}}{d\bar{w}} \right)^{\bar{h}_{\mathcal{O}}} \mathcal{O}(z, \bar{z}) \quad (3.5)$$

with $(h_{\mathcal{O}}, \bar{h}_{\mathcal{O}})$, the conformal weights of \mathcal{O} . $G_n^{\Upsilon}(x)$ can be easily accessed from correlation functions on the cylinder under the conformal maps in eq. (3.4) [41],

$$G_n^{\Upsilon}(x) = n^{-2n(h_{\Upsilon} + \bar{h}_{\Upsilon})} \frac{\langle \prod_{j=1}^n \Upsilon(w_j^-) \Upsilon^\dagger(w_j^+) \rangle_{\text{cyl}}}{\langle \Upsilon(w_1^-) \Upsilon^\dagger(w_1^+) \rangle_{\text{cyl}}^n}. \quad (3.6)$$

where w_j^\pm are the points corresponding to z_j^\pm through the map $w(z)$

$$w_j^- = \frac{\pi}{n}((x-1) + 2j), \quad w_j^+ = \frac{\pi}{n}(-(x+1) + 2j), \quad j = 1, 2, \dots, n. \quad (3.7)$$

3.2 Entanglement asymmetry in CFT

In this subsection, let's mimic the idea of the useful strategy before obtaining $g_n(\alpha, x)$. In the free compact boson CFT, the *charged moments* can be studied in a usual way like the process of computing symmetry resolution of entanglement entropy.

Firstly, we consider the ground state case. Let's briefly review the study before, we can regard $\text{Tr}(\rho_A^n e^{i\alpha Q_A})$ as a partition function in the n -sheet Riemann surface \mathcal{R}_n with an inserted Aharonov-Bohm flux α . In a similar way, $\text{Tr}(\prod_{j=1}^n \rho_A e^{i\alpha_{j,j+1} Q_A})$ can be seen as a partition function in the n -sheet Riemann surface \mathcal{R}_n with the j -th sheet and $j+1$ -th sheet inserted Aharonov-Bohm flux $\alpha_{j,j+1}$. It's easy to understand that a twisted boundary condition corresponds to the insertion of a flux. We can introduce a local operator $\mathcal{V}_{\alpha_{j,j+1}}$ to encode these twisted boundary conditions [7, 10]. If A is an interval $[u, v]$, we can obtain the following relation [42]

$$e^{i\alpha_{j,j+1} Q_A} = \mathcal{V}_{\alpha_{j,j+1}}(u, 0) \mathcal{V}_{-\alpha_{j,j+1}}(v, 0). \quad (3.8)$$

Moreover, one can precisely identity

$$\text{Tr}(\prod_{j=1}^n \rho_I e^{i\alpha_{j,j+1} Q_A}) = \langle \prod_{j=1}^n e^{i\alpha_{j,j+1} Q_A} \rangle_{\mathcal{R}_n} = \langle \prod_{j=1}^n \mathcal{V}_{\alpha_{j,j+1}}(u, 0) \mathcal{V}_{-\alpha_{j,j+1}}(v, 0) \rangle_{\mathcal{R}_n}. \quad (3.9)$$

Refer to the result in the last section eq. (3.3), we similarly have

$$\text{Tr}(\prod_{j=1}^n \rho_{\Upsilon} e^{i\alpha_{j,j+1} Q_A}) = \langle \prod_{j=1}^n \mathcal{V}_{\alpha_{j,j+1}}(u, 0) \mathcal{V}_{-\alpha_{j,j+1}}(v, 0) \Upsilon(z_j^-) \Upsilon^\dagger(z_j^+) \rangle_{\mathcal{R}_n}. \quad (3.10)$$

Therefore, $g_n^{\Upsilon}(\alpha, x)$ can be computed as

$$g_n^{\Upsilon}(\alpha, x) = \frac{\langle \prod_{j=1}^n \mathcal{V}_{\alpha_{j,j+1}}(u, 0) \mathcal{V}_{-\alpha_{j,j+1}}(v, 0) \psi(z_j^-) \psi^\dagger(z_j^+) \rangle_{\mathcal{R}_n}}{\langle \prod_{j=1}^n \Upsilon(z_j^-) \Upsilon^\dagger(z_j^+) \rangle_{\mathcal{R}_n}}. \quad (3.11)$$

Through the conformal transformation defined in eq. (3.4), all the correlation functions in eq. (3.11) can be mapped to correlators on the cylinder. Furthermore, all powers of $(\frac{dz}{dw})$ cancel out in this mapping. Consequently, we can write $g_n(\boldsymbol{\alpha}, x)$ as

$$g_n^\Upsilon(\boldsymbol{\alpha}, x) = \frac{\langle \prod_{j=1}^n \mathcal{V}_{\alpha_{j,j+1}}(i\infty) \mathcal{V}_{-\alpha_{j,j+1}}(-i\infty) \Upsilon(w_j^-) \Upsilon^\dagger(w_j^+) \rangle_{\text{cyl}}}{\langle \prod_{j=1}^n \Upsilon(w_j^-) \Upsilon^\dagger(w_j^+) \rangle_{\text{cyl}}}. \quad (3.12)$$

It's a universal CFT expression written by correlation functions for the charged moments using the replica trick, which is the bridge to the entanglement asymmetry in CFT. We will use the equation above for two types of excited states in CFT. Detailed analytic computations will be discussed in the next section.

4 Excited states in the free compact boson CFT

In this section and the following part, we will focus on the entanglement asymmetry in the free compact boson CFT.

The theory of free compact bosonic field $\varphi(z, \bar{z})$ with Euclidean action

$$\mathcal{A}[\varphi] = \frac{1}{8\pi} \int dz d\bar{z} \partial_z \varphi \partial_{\bar{z}} \varphi \quad (4.1)$$

is a CFT with a central charge $c = 1$. This theory has two types of primary fields and the first type is the vertex operators

$$V_{\alpha, \bar{\alpha}} =: e^{i(\alpha\phi + \bar{\alpha}\bar{\phi})} : \quad (4.2)$$

where $\phi, \bar{\phi}$ are chiral and anti-chiral portions of the bosonic field: $\varphi(z, \bar{z}) = \phi(z) + \bar{\phi}(\bar{z})$, with the conformal weight $(h, \bar{h}) = \left(\frac{\alpha^2}{2}, \frac{\bar{\alpha}^2}{2}\right)$ consisting of the holomorphic and the anti-holomorphic sectors. Another primary operator is the current operator or the derivative operator $J = i\partial\phi$. For computing easily, we assume holomorphic field $\bar{\phi} = 0$.

Considering that the conserved current is proportional to $\partial_x\phi$, the charge operator in the interval A is

$$Q_A = \frac{1}{2\pi} \int_A dx \partial_x \varphi = \frac{1}{2\pi} (\varphi(v) - \varphi(u)). \quad (4.3)$$

Under the inspection of eq. (3.8), the local operator mentioned above $\mathcal{V}_{\alpha_{j,j+1}}$ is implemented by the vertex operator

$$\mathcal{V}_{\alpha_{j,j+1}} = V_{\frac{\alpha_{j,j+1}}{2\pi}} \equiv e^{\frac{i\alpha_{j,j+1}}{2\pi}\varphi}, \quad (4.4)$$

with the conformal weight $(h_{\alpha_{j,j+1}}, \bar{h}_{\alpha_{j,j+1}}) = \left(\frac{1}{2}\left(\frac{\alpha_{j,j+1}}{2\pi}\right)^2, \frac{1}{2}\left(\frac{\alpha_{j,j+1}}{2\pi}\right)^2\right)$.

During the calculation, it was found that we can't achieve $\text{Tr}(\prod_{j=1}^n \rho_A e^{i\alpha_{j,j+1}Q_A})$ straightly. For the total entanglement, the ratio of moments eq. (3.2) is universal and can be calculated in CFT without any input from the model [40]. Inspired by it, we can define the following ratio of charged moments

$$G_n^\Upsilon(\boldsymbol{\alpha}, x) = \frac{\text{Tr}(\prod_{j=1}^n \rho_\Upsilon e^{i\alpha_{j,j+1}Q_A})}{\text{Tr}(\prod_{j=1}^n \rho_I e^{i\alpha_{j,j+1}Q_A})}, \quad (4.5)$$

which is also independent and universal of any microscopic details. Applying the same technique as above, we can rewrite it as

$$G_n^\Upsilon(\boldsymbol{\alpha}, x) = \frac{\langle \prod_{j=1}^n \mathcal{V}_{\alpha_{j,j+1}}(i\infty) \mathcal{V}_{-\alpha_{j,j+1}}(-i\infty) \Upsilon(w_j^-) \Upsilon^\dagger(w_j^+) \rangle_{\text{cyl}}}{\langle \prod_{j=1}^n \mathcal{V}_{\alpha_{j,j+1}}(i\infty) \mathcal{V}_{-\alpha_{j,j+1}}(-i\infty) \rangle_{\text{cyl}}}, \quad (4.6)$$

which will be computed in the following part. Notice that at $\alpha = 0$, $G_n^\Upsilon(0, x) = G_n^\Upsilon(x)$. The observation suggests to define another ratio

$$\begin{aligned} \frac{G_n^\Upsilon(\alpha, x)}{G_n^\Upsilon(0, x)} &= \frac{\text{Tr}(\prod_{j=1}^n \rho_\Upsilon e^{i\alpha_{j,j+1} Q_A}) \text{Tr}(\rho_I^n)}{\text{Tr}(\prod_{j=1}^n \rho_I e^{i\alpha_{j,j+1} Q_A}) \text{Tr}(\rho_\Upsilon^n)} = \frac{g_n^\Upsilon(\alpha, x)}{g_n^I(\alpha, x)} \\ &= \frac{\langle \prod_{j=1}^n \mathcal{V}_{\alpha_{j,j+1}}(i\infty) \mathcal{V}_{-\alpha_{j,j+1}}(-i\infty) \Upsilon(w_j^-) \Upsilon^\dagger(w_j^+) \rangle_{\text{cyl}}}{\langle \prod_{j=1}^n \mathcal{V}_{\alpha_{j,j+1}}(i\infty) \mathcal{V}_{-\alpha_{j,j+1}}(-i\infty) \rangle_{\text{cyl}} \langle \prod_{j=1}^n \Upsilon(w_j^-) \Upsilon^\dagger(w_j^+) \rangle_{\text{cyl}}} \end{aligned} \quad (4.7)$$

From the analysis above, it's of most importance to get $G_n^\Upsilon(\alpha, x)$. In this section, we will discuss how to get $G_n^\Upsilon(\alpha, x)$ with two types of excited states in the free compact boson CFT.

Special attention needs to be paid to the property of the excited state. If the excited state $|\Upsilon\rangle$ is an eigenstate of Q , then $[\rho_A, Q_A] = 0$. Thus the a state like $|V_\beta\rangle$ and $|J\rangle$ will lead to a vanishing entanglement asymmetry. Excited states we will consider must not being eigenstates of Q . These state satisfy $[\rho_A, Q_A] \neq 0$, so their entanglement asymmetries aren't zero.

Regarding with the above discussions, we will calculate $g_2^\Upsilon(x)$ for two kinds of excited states, i.e. $|\Psi\rangle = |V_\beta\rangle + |V_{-\beta}\rangle$ and $|\Phi\rangle = |V_\beta\rangle + |J\rangle$. It is not hard to extend our results to other kinds of excited states.

4.1 Excited state I: $|\Psi\rangle = |V_\beta\rangle + |V_{-\beta}\rangle$

In this subsection, we will focus on the computation of $g_2^\Psi(x)$, with $|\Psi\rangle = |V_\beta\rangle + |V_{-\beta}\rangle$. which is the key ingredient of the Rényi entanglement asymmetry.

$$\begin{aligned} |\Psi\rangle \langle \Psi| &= (|V_\beta\rangle + |V_{-\beta}\rangle)(\langle V_\beta| + \langle V_{-\beta}|) \\ &= |V_\beta\rangle \langle V_\beta| + |V_\beta\rangle \langle V_{-\beta}| + |V_{-\beta}\rangle \langle V_\beta| + |V_{-\beta}\rangle \langle V_{-\beta}|. \end{aligned} \quad (4.8)$$

We know that the correlation function of vertex operators $\langle V_{\alpha_1} V_{\alpha_2} \dots V_{\alpha_N} \rangle$ isn't zero, only if $\sum_{i=1}^N \alpha_i = 0$. Taking this neutral condition into account, we find there are only 6 terms contribute

$$\begin{aligned} G_2^\Psi(\alpha, x) &= F_{\beta, \beta, -\beta, -\beta} + F_{-\beta, -\beta, \beta, \beta} + F_{\beta, -\beta, \beta, -\beta} \\ &\quad + F_{-\beta, \beta, -\beta, \beta} + F_{\beta, -\beta, -\beta, \beta} + F_{-\beta, \beta, \beta, -\beta} \end{aligned} \quad (4.9)$$

where

$$F_{\beta, \beta, -\beta, -\beta} = \frac{\langle \mathcal{V}_\alpha(i\infty) \mathcal{V}_{-\alpha}(-i\infty) V_\beta(w_1^-) V_\beta(w_1^+) \mathcal{V}_{-\alpha}(i\infty) \mathcal{V}_\alpha(-i\infty) V_{-\beta}(w_2^-) V_{-\beta}(w_2^+) \rangle_{\text{cyl}}}{\langle \mathcal{V}_\alpha(i\infty) \mathcal{V}_{-\alpha}(-i\infty) \mathcal{V}_{-\alpha}(i\infty) \mathcal{V}_\alpha(-i\infty) \rangle_{\text{cyl}}}. \quad (4.10)$$

The subscript of the function F indicates the order of the corresponding vertex operator appearing in the correlator. The explicit expressions of other terms in eq. (4.9) can be written down in a similar way. Here and in the following, we are using the notation $\alpha \equiv \alpha_{1,2} = -\alpha_{2,1}$.

We know that the correlation functions of an arbitrary number of vertex operators on the cylinder can be given by elementary methods [43]

$$\langle V_{\alpha_1}(z_1) \dots V_{\alpha_n}(z_n) \rangle_{\text{cyl}} = \prod_{i < j} \left(2 \sin \frac{z_i - z_j}{2} \right)^{\alpha_i \alpha_j}. \quad (4.11)$$

In the following, we plan to calculate $G_2^\Psi(\alpha, x)$, referring to this equation. We find that the computation is complicated but straightforward and the details of the calculation are presented in appendix A. Finally, the Rényi entanglement asymmetry with index $n = 2$ is

$$\Delta S_A^{(2)}(\rho_\Psi) = -\log \frac{a_1 \sin^2(2\pi\beta) + 2b_1 \pi^2 \beta^2}{2\pi^2 \beta^2 (2a_1 + b_1)}. \quad (4.12)$$

with $a_1 = (2 \cot(\frac{\pi x}{2}))^{-2\beta^2}$ and $b_1 = 2(\sin \pi x)^{-2\beta^2} + 2(2 \tan \frac{\pi x}{2})^{-2\beta^2}$.

4.2 Excited state II: $|\Phi\rangle = |V_\beta\rangle + |J\rangle$

In this subsection, we consider another type of excited state, which is the superposition of the vertex operator and the derivative operator i.e. $|\Phi\rangle = |V_\beta\rangle + |J\rangle$. In contrast to the last subsection, a similar but different way will be used. Now we have

$$\begin{aligned} |\Phi\rangle \langle\Phi| &= (|V_\beta\rangle + |J\rangle)(\langle V_\beta| + \langle J|) \\ &= |V_\beta\rangle \langle V_\beta| + |V_\beta\rangle \langle J| + |J\rangle \langle V_\beta| + |J\rangle \langle J|. \end{aligned} \quad (4.13)$$

For simplicity, we will still focus on the case $n = 2$ and higher n can be computed similarly. We have

$$\begin{aligned} G_2^\Phi(\alpha, x) &= F_{\beta, -\beta, \beta, -\beta} + F_{J, -\beta, \beta, J^\dagger} + F_{\beta, J^\dagger, J, -\beta} \\ &\quad + F_{J, J^\dagger, \beta, -\beta} + F_{\beta, -\beta, J, J^\dagger} + F_{J, J^\dagger, J, J^\dagger}. \end{aligned} \quad (4.14)$$

where

$$F_{\beta, -\beta, J, J^\dagger} = \frac{\langle \mathcal{V}_\alpha(i\infty) \mathcal{V}_{-\alpha}(-i\infty) V_\beta(w_1^-) V_{-\beta}(w_1^+) \mathcal{V}_{-\alpha}(i\infty) \mathcal{V}_\alpha(-i\infty) J(w_2^-) J^\dagger(w_2^+) \rangle_{\text{cyl}}}{\langle \mathcal{V}_\alpha(i\infty) \mathcal{V}_{-\alpha}(-i\infty) \mathcal{V}_{-\alpha}(i\infty) \mathcal{V}_\alpha(-i\infty) \rangle_{\text{cyl}}}. \quad (4.15)$$

According to the rules of our notation, it's easy to write down the explicit expression of other terms in the equation above.

Since the direct calculation of the correlation functions of vertex and derivative operators is usually not an easy task, the standard and useful trick is [42]

$$J(z) = i\partial\phi(z) = \frac{1}{\epsilon} \partial_z V_\epsilon(z)|_{\epsilon=0} \quad (4.16)$$

We can use this to calculate the various correlation functions. The calculation is easy and straightforward and we report the final results in appendix B. Adding these results together, one can get $G_2^\Phi(\alpha, x)$ and hence $g_2^\Phi(x)$. Finally, the Rényi entanglement asymmetry $\Delta S_A^{(2)}(\rho_\Phi)$ is given by

$$\Delta S_A^{(2)}(\rho_\Phi) = -\log \frac{2a_2 \sin^2(\pi\beta) + b_2 \pi^2 \beta^2}{\pi^2 \beta^2 (2a_2 + b_2)} \quad (4.17)$$

with

$$a_2 = 2^{-2-\beta^2} \left(-\sec\left(\frac{\pi x}{2}\right)\right)^{\beta^2} \left(\beta^2 \cot^2\left(\frac{\pi x}{2}\right) + \sec^2\left(\frac{\pi x}{2}\right)\right) \quad (4.18)$$

and

$$\begin{aligned} b_2 &= 2^{-2-\beta^2} \left(\csc\left(\frac{\pi x}{2}\right)\right)^{\beta^2} \left(\csc^2\left(\frac{\pi x}{2}\right) + \beta^2 \tan^2\left(\frac{\pi x}{2}\right)\right) + 2^{-3-\beta^2} (2 - 3\beta^2 + \beta^2(\cos(\pi x) + \\ &\quad 2 \sec^2\left(\frac{\pi x}{2}\right)) \left(\sin\left(\frac{\pi x}{2}\right)\right)^{-2-\beta^2} + (\csc(\pi x))^2 \beta^2 + 2^{-6} (7 + \cos(2\pi x))^2 \csc^4(\pi x) \end{aligned} \quad (4.19)$$

In this section, we give the strategy for how to compute the Rényi entanglement asymmetry $\Delta S_A^{(2)}$ and worked out the exact results for $n = 2$. Moreover, it's not too hard to extend our result for $n > 2$ and for other types of excited states with non-vanishing Rényi entanglement asymmetry.

5 Numerical tests

In this section, we will make some numerical tests of the universal CFT computations obtained in previous sections [44–46]. Based on the calculations above, we plan to numerically calculate the

Bosonization dictionary	Boson operator	Fermion operator	Filling in momentum space
Ground state	1	1	○ ○ ○ ● ● ● ● ● ● ● ● ● ○ ○
Particle state	$e^{i\phi}$	Ψ_R^+	○ ○ ○ ● ● ● ● ● ● ● ● ○ ○ ○
Hole state	$e^{-i\phi}$	Ψ_R	○ ○ ○ ● ● ● ● ● ● ● ○ ○ ○ ○ ○
Particle-hole state	$i\partial\phi$	$\Psi_R^+ \Psi_R$	○ ○ ○ ● ● ● ● ● ● ○ ● ● ○ ○

Figure 2: Bosonization dictionary for some low-energy excitations of a free-fermion chain with the Hamiltonian $H = -\frac{1}{4} \sum_{j=1}^L (\sigma_j^x \sigma_{j+1}^x + \sigma_j^y \sigma_{j+1}^y - h \sigma_j^z)$.

individual terms occur in the original expressions of G_2^Ψ and G_2^Φ (c.f. eq. (4.9) and eq. (4.14)). We will take the XX spin chain model with periodic boundary conditions as an concrete lattice realization of our free compact boson CFT. As is well known, the XX spin chain is described by the following Hamiltonian [47]

$$H = -\frac{1}{4} \sum_{j=1}^L (\sigma_j^x \sigma_{j+1}^x + \sigma_j^y \sigma_{j+1}^y - h \sigma_j^z), \quad (5.1)$$

where $\sigma_j^{x,y,z}$ are the Pauli matrices acting on the j -th site. After a Jordan-Wigner transformation and Fourier transformation, it can be diagonalized and the eigenstates of the Hamilton are described by a set of momenta K , $|K\rangle = \prod_{k \in K} b_k^\dagger |0\rangle$. See appendix C for details.

If we prepare the spin chain in the state $\rho = |K\rangle \langle K|$ and then consider the case where the subsystem A consists of l continuous sites, we write the Majorana correlation matrix as

$$\text{Tr}(\rho a_i a_j) = \delta_{ij} + \Gamma_{ij}^K, \quad (5.2)$$

with $\Gamma^K \in \mathcal{M}_{2l}(\mathbb{C})$. Γ^K is a block matrix with elements given by

$$\Gamma_{ij}^K = T_{j-i}^K, \quad T_n^K = \begin{pmatrix} f_n^K & g_n^K \\ -g_n^K & f_n^K \end{pmatrix}, \quad (5.3)$$

In eq. (4.9) and eq. (4.14), we find that there are Hermite and non-Hermite terms. For Hermite terms, f_n^K and g_n^K have the following form

$$\begin{aligned} f_n^K &= \frac{1}{L} \sum_{k \in K} e^{i\phi_k n} - \frac{1}{L} \sum_{k \notin K} e^{-i\phi_k n}, \\ g_n^K &= -\frac{i}{L} \sum_{k \in K} e^{-i\phi_k n} + \frac{i}{L} \sum_{k \notin K} e^{i\phi_k n}. \end{aligned} \quad (5.4)$$

Moreover, their CFT predictions have been tested with the concrete lattice calculations in the XX spin chain and performed well in [9]. Therefore, all we need is to check whether the CFT results of the non-Hermite parts are in perfect agreement with the exact numerical calculations.

The low-lying states are excitations of holes and particles below or above the Fermi Sea. The correspondences of the vertex and derivative operators will be found by recalling the bosonization dictionary, which helps us a lot in providing the numerical tests in the two excited states discussed in the previous section. Some examples of the correspondence between CFT operators and the low-energy excitations in XX spin chain are shown in Fig. 2.

5.1 Excited state I: $|\Psi\rangle = |V_\beta\rangle + |V_{-\beta}\rangle$

For simplicity, we assume that $\beta = 1$. The vertex operator $V_{-1} = e^{-i\phi}$ corresponds to a hole excitation and $V_1 = e^{i\phi}$ corresponds to a particle excitation, at the Fermi momentum [40]. Because of $n_F = \frac{L}{2}$ and its corresponding $\{\pm\frac{1}{2}, \pm\frac{3}{2}, \dots, \pm\frac{n_F-1}{2}\}$, the relations of these two states is

$$|V_1\rangle = b_q^\dagger b_{q'}^\dagger |V_{-1}\rangle \quad q = \frac{L}{4} - \frac{1}{2}, q' = \frac{L}{4} + \frac{1}{2}. \quad (5.5)$$

Non-Hermite terms $|V_\beta\rangle \langle V_{-\beta}|$ and $|V_{-\beta}\rangle \langle V_\beta|$ appearing in eq. (4.9) cannot be viewed as some density matrices, since their traces are zero. To deal with this kind of object, we introduce the operator S satisfying $S^2 = I$ and $\langle V_1|S|V_{-1}\rangle \neq 0$ to define a fake density matrix

$$\rho^S = \frac{S|V_{-1}\rangle \langle V_1|}{\langle V_1|S|V_{-1}\rangle} \quad (5.6)$$

The corresponding Majorana matrix can be defined in the following way [48]

$$\Gamma_{ij}^S = \text{Tr}(\rho^S a_i a_j) - \delta_{ij} = \frac{\langle V_1|S a_i a_j|V_{-1}\rangle}{\langle V_1|S|V_{-1}\rangle} - \delta_{ij}, \quad (5.7)$$

For different non-Hermitian terms, we should construct an appropriate operator S , with the conditions mentioned above being satisfied. For the term $|V_{-1}\rangle \langle V_1|$, we could choose the S operator as

$$S = \sigma_n^x \sigma_{n+1}^y = -i a_{2n-1} a_{2n+1} = i(c_n - c_n^\dagger)(c_{n+1} - c_{n+1}^\dagger). \quad (5.8)$$

Other forms of S fulfilling the conditions mentioned before are also workable. Refer to eq. (5.8), we have

$$\begin{aligned} \langle V_1|S|V_{-1}\rangle &= i \langle c_n^\dagger c_{n+1}^\dagger b_q b_{q'} \rangle_{V_1} = \frac{i}{L} \sum_{k, k' \in \Omega} e^{-i\phi_k n - i\phi_{k'}(n+1)} \langle b_k^\dagger b_{k'}^\dagger b_q b_{q'} \rangle_{V_1} \\ &= \frac{i}{L} [e^{-i\phi_q n - i\phi_{q'}(n+1)} - e^{-i\phi_{q'} n - i\phi_q(n+1)}] \equiv i f_0(n, n+1). \end{aligned} \quad (5.9)$$

Where $c_n = \frac{1}{\sqrt{L}} \sum_{k \in \Omega} b_k e^{i\phi_k n}$ with $\phi_k = \frac{2\pi k}{L}$.

Similarly, the Majorana matrix Γ^S is a block matrix with elements given by

$$\Gamma_{r,s}^S = T_{r,s}^S, \quad T_{r,s}^S = \begin{pmatrix} f_1(r, s) & g_1(r, s) \\ g_2(r, s) & f_2(r, s) \end{pmatrix}. \quad (5.10)$$

The explicit form of the functions f_1, f_2, g_1 and g_2 can be found in appendix D.

We numerically compute the α -dependence of the normalized $F_{\beta, \beta, -\beta, -\beta}$ for $\beta = 1$, i.e. $F_{1,1,-1,-1}/F_{1,1,-1,-1}^{\alpha=0}$. The numerical data are shown in Fig. 3. As a comparison, the following analytical predictions

$$\frac{F_{1,1,-1,-1}}{F_{1,1,-1,-1}^{\alpha=0}} = e^{2i\alpha} = \cos(2\alpha) + i \sin(2\alpha), \quad (5.11)$$

are also plot as the full line in Fig. 3.

Our numerical data should converge to the CFT result in eq. (5.11), in the limit $L \rightarrow \infty$. As shown in the figure, the agreement between CFT prediction and numerical data is extremely excellent for all $\alpha \in [-\pi, \pi)$. Although not showed here, we find that for $\beta = -1$, the CFT prediction and the numerical result also match very well.

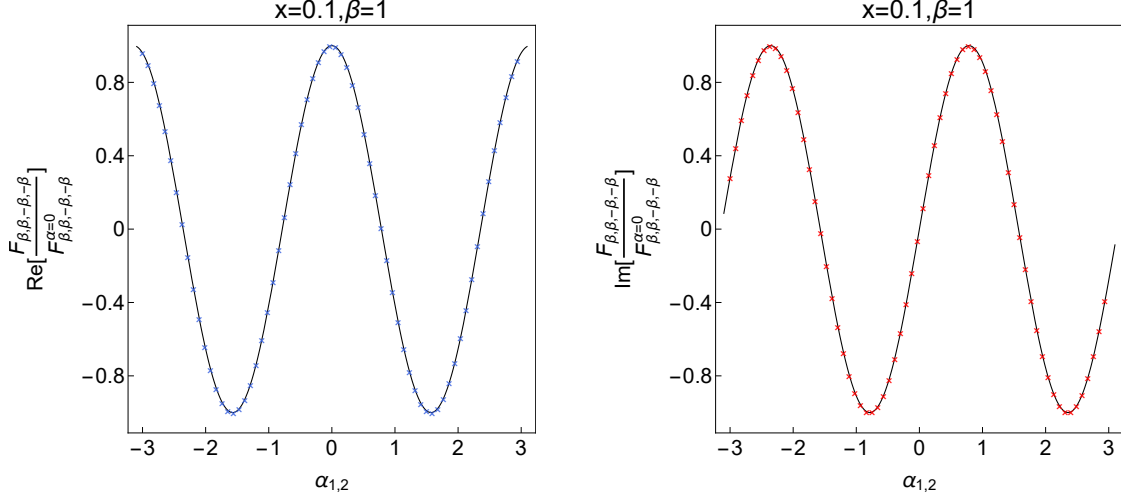


Figure 3: Numerical result of $F_{\beta,\beta,-\beta,-\beta}/F_{\beta,\beta,-\beta,-\beta}^{\alpha=0}$ in the XX spin chain. The full lines are the CFT results in eq. (5.11). Here we consider $x = 0.1, \beta = 1, n = 2$ with total length $L = 1000$ and subsystem size $l = 100$. As shown in the figure, the agreement is fairly well for $\alpha_{1,2} \in [-\pi, \pi]$

5.2 Excited state II: $|\Phi\rangle = |V_\beta\rangle + |J\rangle$

In this subsection, we will discuss the numerical test in the excited state $|\psi\rangle = |V_\beta\rangle + |J\rangle$. As discussed in the previous subsection, for non-Hermitian terms like $|V_\beta\rangle\langle J|$, we should choose an appropriate operator S to define the corresponding fake density matrix. For simplicity, we take $\beta = 1$ again. For the non-Hermitian $|V_1\rangle\langle J|$ and $|J\rangle\langle V_1|$, we should find out the operator S . The first step is to find the relationship between $|V_1\rangle$ and $|J\rangle$. The derivative operator J corresponds to a right-moving particle-hole excitation so that we can write [40]

$$|V_1\rangle = b_q^\dagger |J\rangle, \quad q = \frac{L}{4} - \frac{1}{2} \quad (5.12)$$

In this situation, we could choose S as

$$S = a_{2n-1} = i(c_n - c_n^\dagger) \quad (5.13)$$

The corresponding Majorana matrix is

$$\Gamma_{ij}^S = \frac{\langle V_1 | S a_i a_j | J \rangle}{\langle V_1 | S | J \rangle} - \delta_{ij} \quad (5.14)$$

where

$$\langle V_1 | S | J \rangle = -i \sum_{k \in \Omega} e^{-i\phi_k n} \langle b_k^\dagger b_q \rangle_{V_1} = -\frac{i}{\sqrt{L}} e^{-i\phi_q n} \equiv -i g_0(n) \quad (5.15)$$

In this case, the Majorana matrix Γ^S is a block matrix with elements given by

$$\Gamma_{r,s}^S = \begin{pmatrix} \tilde{f}_1(r, s) & \tilde{g}_1(r, s) \\ \tilde{g}_2(r, s) & \tilde{f}_2(r, s) \end{pmatrix}. \quad (5.16)$$

The explicit form of Γ_{ij}^S can be found in appendix D.

The CFT predictions of the normalized $F_{\beta,J^\dagger,J,-\beta}$ for $\beta = 1$, i.e. $F_{1,J^\dagger,J,-1}/F_{1,J^\dagger,J,-1}^{\alpha=0}$ is

$$\frac{F_{1,J^\dagger,J,-1}}{F_{1,J^\dagger,J,-1}^{\alpha=0}} = e^{i\alpha} = \cos \alpha + i \sin \alpha, \quad (5.17)$$

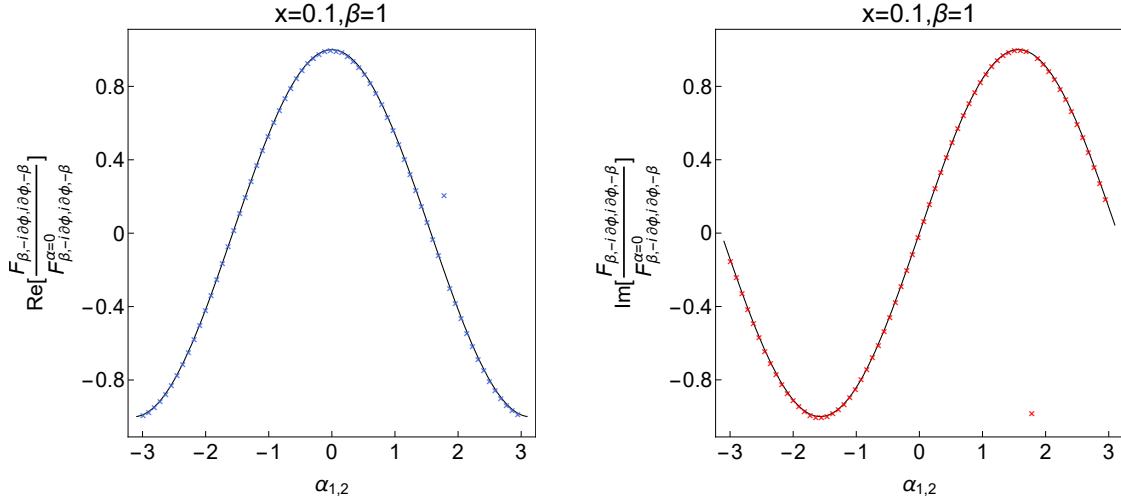


Figure 4: Numerical result of $F_{\beta, -i\partial\phi, i\partial\phi, -\beta} / F_{\beta, -i\partial\phi, i\partial\phi, -\beta}^{\alpha=0}$ in the XX spin chain. The full lines are the CFT results in eq. (5.17). Here we consider $x = 0.1, \beta = 1, n = 2$ with total length $L = 1000$ and subsystem size $l = 100$. Again, the CFT prediction and the numerical result also match extremely well for $\alpha_{1,2} \in [-\pi, \pi)$.

We numerically compute $F_{1, J^\dagger, J, -1} / F_{1, J^\dagger, J, -1}^{\alpha=0}$ and the data are shown in Fig. 4 as dots. As shown in this figure, the agreement between CFT prediction and numerical result is perfect for all $\alpha \in [-\pi, \pi)$.

6 Conclusion

In this manuscript, we study the Rényi entanglement asymmetry of two excited states in the free compact boson CFT and the underlying lattice model.

Using the replica method, we obtain a universal CFT expression written by the correlation functions for the charge moments. We mention that the entanglement asymmetry of an eigenstate of Q will vanish. Thus we construct two types of excited states: $|\Psi\rangle = |V_\beta\rangle + |V_{-\beta}\rangle$ and $|\Phi\rangle = |V_\beta\rangle + |J\rangle$, which are not the eigenstates of the charge. Considering the characteristics of vertex and current operators, we are able to calculate the correlation functions involving vertex and current operators. As a concrete example, we obtained the exact results for the Rényi index $n = 2$ from the CFT computation.

The numerical method of computing the charged moments with non-Hermitian fake RDMS has never been studied before. In this paper, we propose a efficient way to treat them numerically. The CFT predictions are in perfect agreement with the exact numerical calculations, which confirms our numerical method.

In this paper, we only consider Rényi entanglement asymmetry with index $n = 2$, it would be very interesting to derive a formula for general n and analytical continue to $n = 1$ to obtain the entanglement asymmetry. It will also be interesting the consider other kinds of excited states and the content of operator S should be change to adapt this modification.

Acknowledgments

A Correlation functions of vertex operators

The most important basis of the appendix is eq. (A.1)

$$\langle V_{\alpha_1}(z_1)\dots V_{\alpha_n}(z_n)\rangle_{\text{cyl}} = \prod_{i<j} \left(2 \sin \frac{z_i - z_j}{2}\right)^{\alpha_i \alpha_j}. \quad (\text{A.1})$$

Using the above formula, it's straightforward to obtain

$$\begin{aligned} F_{\beta,\beta,-\beta,-\beta} &= (2 \cot(\frac{\pi x}{2}))^{-2\beta^2} e^{2i\beta\alpha}, \\ F_{\beta,-\beta,\beta,-\beta} &= (\sin(\pi x))^{-2\beta^2}, \\ F_{\beta,-\beta,-\beta,\beta} &= (2 \tan(\frac{\pi x}{2}))^{-2\beta^2}. \end{aligned} \quad (\text{A.2})$$

The additional three terms in eq. (4.9) can easily be obtained from the results above with the replacement $\beta \rightarrow -\beta$,

$$\begin{aligned} F_{-\beta,-\beta,\beta,\beta} &= (2 \cot(\frac{\pi x}{2}))^{-2\beta^2} e^{-2i\beta\alpha}, \\ F_{-\beta,\beta,-\beta,\beta} &= (\sin(\pi x))^{-2\beta^2}, \\ F_{-\beta,\beta,\beta,-\beta} &= (2 \tan(\frac{\pi x}{2}))^{-2\beta^2}. \end{aligned} \quad (\text{A.3})$$

Eventually, adding all the terms together, we obtain $G_2^\Psi(\boldsymbol{\alpha}, x)$

$$G_2^\Psi(\boldsymbol{\alpha}, x) = a_1(e^{2i\beta\alpha} + e^{-2i\beta\alpha}) + b_1 \quad (\text{A.4})$$

with $a_1 = (2 \cot(\frac{\pi x}{2}))^{-2\beta^2}$ and $b_1 = 2(\sin \pi x)^{-2\beta^2} + 2(2 \tan \frac{\pi x}{2})^{-2\beta^2}$. Then $g_2^\Psi(\boldsymbol{\alpha}, x)$ is given

$$g_2^\Psi(\boldsymbol{\alpha}, x) = \frac{2a_1 \cos(2\beta\alpha) + b_1}{2a_1 + b_1}. \quad (\text{A.5})$$

Here we have used the fact that $g_2^I(\boldsymbol{\alpha}, x) = 1$ since $[\rho_I, Q_A] = 0$.

After the Fourier transform, we obtain the final result

$$g_2^\Psi(x) = \frac{a_1 \sin^2(2\pi\beta) + 2b_1\pi^2\beta^2}{2\pi^2\beta^2(2a_1 + b_1)}. \quad (\text{A.6})$$

B Correlation functions of vertex and derivative operators

The strategy to compute the correlation functions involving derivative operators is to use the following trick to represent the current operator as a vertex operator

$$(i\partial\phi)(z) = \frac{1}{\epsilon} \partial_z V_\epsilon(z)|_{\epsilon=0} \quad (\text{B.1})$$

Then terms appearing in eq. (4.14) can be computed easily. For example,

$$\begin{aligned} F_{\beta,-\beta,J,J^\dagger} &= \frac{\partial_{w_2^-, w_2^+}}{\epsilon_1 \epsilon_2} \frac{\langle \mathcal{V}_\alpha(i\infty) \mathcal{V}_{-\alpha}(-i\infty) V_\beta(w_1^-) V_{-\beta}(w_1^+) \mathcal{V}_{-\alpha}(i\infty) \mathcal{V}_\alpha(-i\infty) V_{\epsilon_1}(w_2^-) V_{\epsilon_2}^\dagger(w_2^+) \rangle_{\text{cyl}}}{\langle \mathcal{V}_\alpha(i\infty) \mathcal{V}_{-\alpha}(-i\infty) \mathcal{V}_{-\alpha}(i\infty) \mathcal{V}_\alpha(-i\infty) \rangle_{\text{cyl}}} \Big|_{\epsilon_1, \epsilon_2=0} \\ &= 2^{-2-2\beta^2} (\csc(\frac{\pi x}{2}))^{\beta^2} (\csc^2(\frac{\pi x}{2}) + \beta^2 \tan^2(\frac{\pi x}{2})). \end{aligned} \quad (\text{B.2})$$

Similarly, one can get

$$\begin{aligned}
F_{\beta, J^\dagger, J, -\beta} &= 2^{-2-\beta^2} \left(-\sec\left(\frac{\pi x}{2}\right)\right)^{\beta^2} \left(\beta^2 \cot^2\left(\frac{\pi x}{2}\right) + \sec^2\left(\frac{\pi x}{2}\right)\right) e^{i\alpha\beta}, \\
F_{J, -\beta, \beta, J^\dagger} &= 2^{-2-\beta^2} \left(-\sec\left(\frac{\pi x}{2}\right)\right)^{\beta^2} \left(\beta^2 \cot^2\left(\frac{\pi x}{2}\right) + \sec^2\left(\frac{\pi x}{2}\right)\right) e^{-i\alpha\beta}, \\
F_{J, J^\dagger, \beta, -\beta} &= 2^{-3-\beta^2} (2 - 3\beta^2 + \beta^2(\cos(\pi x) + 2\sec^2\left(\frac{\pi x}{2}\right))) \left(\sin\left(\frac{\pi x}{2}\right)\right)^{-2-\beta^2}, \\
F_{J, J^\dagger, J, J^\dagger} &= 2^{-6} (7 + \cos(2\pi x))^2 \csc^4(\pi x).
\end{aligned} \tag{B.3}$$

In appendix A, we have already obtained the value of $F_{\beta, -\beta, \beta, -\beta} = (\csc(\pi x))^{2\beta^2}$. Adding all these terms together, we find

$$G_2(\boldsymbol{\alpha}, x) = a_2(e^{i\alpha\beta} + e^{-i\alpha\beta}) + b_2. \tag{B.4}$$

where the coefficients a_2 and b_2 are given in eq. (4.18) and eq. (4.19) respectively. Finally, one find that $g_2^\Phi(\alpha, x)$ has the same structure with $g_2^\Psi(\alpha, x)$

$$g_2^\Phi(\alpha, x) = \frac{2a_2 \cos(\beta\alpha) + b_2}{2a_2 + b_2}. \tag{B.5}$$

After the Fourier transform, the final result is obtained

$$g_2^\Phi(x) = \frac{2a_2 \sin^2(\pi\beta) + b_2 \pi^2 \beta^2}{\pi^2 \beta^2 (2a_2 + b_2)} \tag{B.6}$$

C RDMs and Correlation matrices in the XX spin chain

As is well known, the XX spin chain is described by the following Hamiltonian [47]

$$H = -\frac{1}{4} \sum_{j=1}^L (\sigma_j^x \sigma_{j+1}^x + \sigma_j^y \sigma_{j+1}^y - h \sigma_j^z), \tag{C.1}$$

where $\sigma_j^{x,y,z}$ are the Pauli matrices acting on the j -th site.

After a Jordan-Wigner transformation

$$c_j = \left(\prod_{k=1}^{j-1} \sigma_k^z \right) \frac{\sigma_j^x - i \sigma_j^y}{2}, \quad c_j^\dagger = \left(\prod_{k=1}^{j-1} \sigma_k^z \right) \frac{\sigma_j^x + i \sigma_j^y}{2}, \tag{C.2}$$

this spin chain Hamiltonian is mapped to a free fermion Hamiltonian on the lattice

$$H = -\frac{1}{2} \sum_{j=1}^L \left[c_j^\dagger c_{j+1} + c_{j+1}^\dagger c_j - 2h(c_j^\dagger c_j - \frac{1}{2}) \right], \tag{C.3}$$

where c_j^\dagger, c_j are fermionic creation and annihilation operators, satisfying the anticommutation relations $\{c_i, c_j^\dagger\} = \delta_{ij}$. Impose anti-periodic boundary conditions to the fermions, $c_{L+1}^\dagger = -c_1^\dagger, c_{L+1} = -c_1$. For simplicity, we will assume that $h = 0$.

After Fourier transformation

$$b_k = \frac{1}{\sqrt{L}} \sum_{l=1}^L c_l e^{i\phi_k l}, \quad \phi_k \equiv \frac{2\pi k}{L} \tag{C.4}$$

the Hamiltonian can be diagonalized as [49]

$$H = \sum_{k \in \Omega} \epsilon_k (b_k^\dagger b_k - \frac{1}{2}), \quad (\text{C.5})$$

where $\epsilon_k = -\cos k$, and $\Omega = \{\pm \frac{1}{2}, \pm \frac{3}{2}, \dots, \pm \frac{L-1}{2}\}$. The eigenstates of the Hamiltonian can be described by a set of momenta K ,

$$|K\rangle = \prod_{k \in K} b_k^\dagger |0\rangle. \quad (\text{C.6})$$

The ground state is half-filling with fermion number $n_F = \frac{L}{2}$ and is a Fermi sea with Fermi momentum $k_F = \frac{\pi}{2}$. And it's characterized by the set of momenta: $\{\pm \frac{1}{2}, \pm \frac{3}{2}, \dots, \pm \frac{n_F-1}{2}\}$. By removing or adding particles in momentum space close to the Fermi surface, we can obtain low-lying excited states [41]. This model has a $U(1)$ symmetry generated by the conserved charge $Q = \sum_{j=1}^L c_j^\dagger c_j$.

If the subsystem A is made of l contiguous lattice sites, then the RDM of the state $|K\rangle \langle K|$ is given by [46]

$$\rho_A = \det C_A^K \exp \left(\sum_{i,j} \log [((C_A^K)^{-1} - 1)]_{ij} c_i^\dagger c_j \right). \quad (\text{C.7})$$

where the $l \times l$ matrix $[C_A^K]_{m,n} = \langle K | c_m^\dagger c_n | K \rangle$, with $m, n \in A$, is the correlation matrix restricted in A . The elements of C_A^K are given by

$$[C_A^K]_{mn} = \frac{1}{L} \sum_{k \in K} e^{i\phi_k(m-n)}. \quad (\text{C.8})$$

It's convenient to introduce the Majorana fermionic operators [50]

$$a_{2s} = c_s^\dagger + c_s, \quad a_{2s-1} = i(c_s - c_s^\dagger), \quad (\text{C.9})$$

satisfying $\{a_i, a_j\} = 2\delta_{ij}$. For the case of a single interval with l sites of the spin chain in a state $|K\rangle$, the Majorana correlation matrix can obtain

$$\langle a_i a_j \rangle_K = \delta_{ij} + \Gamma_{ij}^K, \quad (\text{C.10})$$

with $\Gamma \in \mathcal{M}_{2l}(\mathbb{C})$:

$$\Gamma^K = \begin{pmatrix} T_0^K & T_1^K & \dots & T_{l-1}^K \\ T_{-1}^K & T_0^K & \dots & T_{l-2}^K \\ \vdots & \vdots & \ddots & \vdots \\ T_{1-l}^K & T_{2-l}^K & \dots & T_0^K \end{pmatrix}, \quad T_n^K = \begin{pmatrix} f_n^K & g_n^K \\ -g_n^K & f_n^K \end{pmatrix}, \quad (\text{C.11})$$

The correlation matrix Γ^K determines the $2^l \times 2^l$ RDM. Moreover, we can also regard $e^{i\alpha Q_A}$ as some RDM with Majorana correlation matrix Γ^α since

$$\begin{aligned} e^{i\alpha Q_A} &= e^{i\alpha \sum_{j=1}^l c_j^\dagger c_j} = \prod_{j=1}^l (e^{i\alpha} c_j^\dagger c_j + c_j c_j^\dagger) \\ &= (1 + e^{i\alpha})^l \prod_{j=1}^l [p_j c_j c_j^\dagger + (1 - p_j) c_j^\dagger c_j], \end{aligned} \quad (\text{C.12})$$

where $p_j = \frac{1}{1+e^{i\alpha}}$. The Majorana correlation matrix Γ^α and Γ^K (cf. (C.11)) have the same structure, but different block matrices [9]

$$f_n^\alpha = 0, \quad g_n^\alpha = \frac{i(1 - e^{i\alpha})}{e^{i\alpha} + 1} \delta_{n,0}. \quad (\text{C.13})$$

In the process of calculation, we will encounter the composition matrices indicated by $\Gamma_i \times \Gamma_j$. It is implicitly defined by [41, 48, 51]

$$\rho_{\Gamma_i} \rho_{\Gamma_j} = \text{tr}(\rho_{\Gamma_i} \rho_{\Gamma_j}) \rho_{\Gamma_i \times \Gamma_j}, \quad (\text{C.14})$$

where

$$\text{tr}(\rho_{\Gamma_i} \rho_{\Gamma_j}) = \sqrt{\left| \frac{1 + \Gamma_i \Gamma_j}{2} \right|}, \quad (\text{C.15})$$

and the product rule is

$$\Gamma_i \times \Gamma_j = 1 - (1 - \Gamma_j)(1 + \Gamma_i \Gamma_j)^{-1}(1 - \Gamma_i). \quad (\text{C.16})$$

By associativity, the trace of the product of arbitrary number of RDMs can be obtained

$$\text{tr}(\rho_{\Gamma_i} \rho_{\Gamma_j} \cdots) = \text{tr}(\rho_{\Gamma_i} \rho_{\Gamma_j}) \text{tr}(\rho_{\Gamma_i \times \Gamma_j} \cdots). \quad (\text{C.17})$$

Based on the formula established above, one can numerically compute the charged moments $Z_n(\alpha)$ eq. (2.8) with Hermitian ρ_A for arbitrary n . Since this method is thoroughly studied in previous literature [9], we will not discuss it here.

D Non-Hermite fake RDMs and Correlation matrices

Considering the characteristics of the Majorana fermionic operators, we have

$$\begin{aligned} a_i a_j &= \begin{pmatrix} a_{2r} \\ a_{2r-1} \end{pmatrix} (a_{2s} a_{2s-1}) \\ &= \begin{pmatrix} (c_r^\dagger + c_r)(c_s^\dagger + c_s) & i(c_r^\dagger + c_r)(c_s^\dagger - c_s) \\ i(c_r^\dagger - c_r)(c_s^\dagger + c_s) & -(c_r^\dagger - c_r)(c_s^\dagger - c_s) \end{pmatrix}. \end{aligned} \quad (\text{D.1})$$

For excited state $|\Psi\rangle = |V_1\rangle + |V_{-1}\rangle$, the S operator we have chosen is $S = -ia_{2n-1}a_{2n+1}$. Then the corresponding Majorana matrix can be computed as

$$\begin{aligned} f_1(r, s) &= f_0(n, n+1)^{-1} (\langle V_1 | c_n^\dagger c_{n+1}^\dagger c_r^\dagger c_s | V_{-1} \rangle + \langle V_1 | c_n^\dagger c_{n+1}^\dagger c_s^\dagger c_r | V_{-1} \rangle \\ &\quad - \langle V_1 | c_n^\dagger c_r^\dagger c_s^\dagger c_{n+1} | V_{-1} \rangle - \langle V_1 | c_{n+1}^\dagger c_r^\dagger c_s^\dagger c_n | V_{-1} \rangle) \end{aligned} \quad (\text{D.2})$$

$$\begin{aligned} f_2(r, s) &= f_0(n, n+1)^{-1} (\langle V_1 | c_n^\dagger c_{n+1}^\dagger c_r^\dagger c_s | V_{-1} \rangle + \langle V_1 | c_n^\dagger c_{n+1}^\dagger c_s^\dagger c_r | V_{-1} \rangle \\ &\quad + \langle V_1 | c_n^\dagger c_r^\dagger c_s^\dagger c_{n+1} | V_{-1} \rangle + \langle V_1 | c_{n+1}^\dagger c_r^\dagger c_s^\dagger c_n | V_{-1} \rangle) \end{aligned} \quad (\text{D.3})$$

$$\begin{aligned} g_1(r, s) &= -if_0(n, n+1)^{-1} (\langle V_1 | c_n^\dagger c_{n+1}^\dagger c_r^\dagger c_s | V_{-1} \rangle - \langle V_1 | c_n^\dagger c_{n+1}^\dagger c_s^\dagger c_r | V_{-1} \rangle \\ &\quad + \langle V_1 | c_n^\dagger c_r^\dagger c_s^\dagger c_{n+1} | V_{-1} \rangle + \langle V_1 | c_{n+1}^\dagger c_r^\dagger c_s^\dagger c_n | V_{-1} \rangle) + \delta_{mn} \end{aligned} \quad (\text{D.4})$$

$$\begin{aligned} g_2(r, s) &= -if_0(n, n+1)^{-1} (-\langle V_1 | c_n^\dagger c_{n+1}^\dagger c_r^\dagger c_s | V_{-1} \rangle + \langle V_1 | c_n^\dagger c_{n+1}^\dagger c_s^\dagger c_r | V_{-1} \rangle \\ &\quad + \langle V_1 | c_n^\dagger c_r^\dagger c_s^\dagger c_{n+1} | V_{-1} \rangle + \langle V_1 | c_{n+1}^\dagger c_r^\dagger c_s^\dagger c_n | V_{-1} \rangle) + \delta_{mn} \end{aligned} \quad (\text{D.5})$$

Let's first consider $\langle V_1 | c_n^\dagger c_{n+1}^\dagger c_r^\dagger c_s | V_{-1} \rangle$. We have

$$\langle V_1 | c_n^\dagger c_{n+1}^\dagger c_r^\dagger c_s | V_{-1} \rangle = \frac{1}{L^2} \sum_{k, k', k_1, k_2 \in \Omega} e^{-i\phi_k n - i\phi_{k'}(n+1) - i\phi_{k_1} r + i\phi_{k_2} s} \langle b_k^\dagger b_{k'}^\dagger b_{k_1}^\dagger b_{k_2} b_q b_{q'} \rangle. \quad (\text{D.6})$$

Here and in the following, $\langle \cdot \rangle$ means the average under the state V_1 . According to the Wick theorem, we have

$$\begin{aligned} \langle b_k^\dagger b_{k'}^\dagger b_{k_1}^\dagger b_{k_2}^\dagger b_q b_{q'} \rangle &= \langle b_{k_1}^\dagger b_{k_2} \rangle (\langle b_{k'}^\dagger b_q \rangle \langle b_k^\dagger b_{q'} \rangle - \langle b_k^\dagger b_q \rangle \langle b_{k'}^\dagger b_{q'} \rangle) \\ &\quad - \langle b_{k'}^\dagger b_{k_2} \rangle (\langle b_k^\dagger b_q \rangle \langle b_{k_1}^\dagger b_{q'} \rangle - \langle b_{k_1}^\dagger b_q \rangle \langle b_k^\dagger b_{q'} \rangle) \\ &\quad + \langle b_k^\dagger b_{k_2} \rangle (\langle b_{k'}^\dagger b_q \rangle \langle b_{k_1}^\dagger b_{q'} \rangle - \langle b_{k_1}^\dagger b_q \rangle \langle b_{k'}^\dagger b_{q'} \rangle) \end{aligned} \quad (\text{D.7})$$

Using $\langle b_k^\dagger b_{k'} \rangle = \delta_{k,k'} \delta_{k \in V_1}$, we obtain

$$\langle V_1 | c_n^\dagger c_{n+1}^\dagger c_r^\dagger c_s | V_{-1} \rangle = \frac{1}{L} \sum_{k \in V_1} [e^{-i\phi_k(r-s)} f_0(n, n+1) - e^{-i\phi_k(n+1-s)} f_0(n, r) + e^{-i\phi_k(n-s)} f_0(n+1, r)]. \quad (\text{D.8})$$

The other terms can be obtained similarly

$$\begin{aligned} \langle V_1 | c_n^\dagger c_{n+1}^\dagger c_s^\dagger c_r | V_{-1} \rangle &= -\frac{1}{L} \sum_{k \in V_1} [e^{-i\phi_k(s-r)} f_0(n, n+1) - e^{-i\phi_k(n+1-r)} f_0(n, s) + e^{-i\phi_k(n-r)} f_0(n+1, s)], \\ \langle V_1 | c_n^\dagger c_r^\dagger c_s^\dagger c_{n+1} | V_{-1} \rangle &= \frac{1}{L} \sum_{k \in V_1} [e^{-i\phi_k(s-(n+1))} f_0(n, r) - e^{-i\phi_k(r-(n+1))} f_0(n, s) + e^{i\phi_k} f_0(r, s)], \\ \langle V_1 | c_n^\dagger c_r^\dagger c_s^\dagger c_{n+1} | V_{-1} \rangle &= -\frac{1}{L} \sum_{k \in V_1} [e^{-i\phi_k(s-n)} f_0(n+1, r) - e^{-i\phi_k(r-n)} f_0(n+1, s) + e^{-i\phi_k} f_0(r, s)]. \end{aligned} \quad (\text{D.9})$$

For excited state $|\Phi\rangle = |V_1\rangle + |J\rangle$, we should choose the S operator as $S = a_{2n-1}$ instead. The corresponding Majorana matrix can be computed as

$$\begin{aligned} \tilde{f}_1(r, s) &= g_0(n)^{-1} (-\langle V_1 | c_r^\dagger c_s^\dagger c_n | J \rangle + \langle V_1 | c_n^\dagger c_r^\dagger c_s | J \rangle + \langle V_1 | c_n^\dagger c_s^\dagger c_r | J \rangle), \\ \tilde{f}_2(r, s) &= g_0(n)^{-1} (\langle V_1 | c_r^\dagger c_s^\dagger c_n | J \rangle + \langle V_1 | c_n^\dagger c_r^\dagger c_s | J \rangle + \langle V_1 | c_n^\dagger c_s^\dagger c_r | J \rangle), \\ \tilde{g}_1(r, s) &= -ig_0(n)^{-1} (\langle V_1 | c_r^\dagger c_s^\dagger c_n | J \rangle + \langle V_1 | c_n^\dagger c_r^\dagger c_s | J \rangle - \langle V_1 | c_n^\dagger c_s^\dagger c_r | J \rangle) + \delta_{rs}, \\ \tilde{g}_2(r, s) &= -ig_0(n)^{-1} (\langle V_1 | c_r^\dagger c_s^\dagger c_n | J \rangle - \langle V_1 | c_n^\dagger c_r^\dagger c_s | J \rangle + \langle V_1 | c_n^\dagger c_s^\dagger c_r | J \rangle) + \delta_{rs}. \end{aligned} \quad (\text{D.10})$$

Now let's compute $\langle V_1 | c_r^\dagger c_s^\dagger c_n | J \rangle$ first

$$\langle V_1 | c_r^\dagger c_s^\dagger c_n | J \rangle = \frac{i}{L^{\frac{3}{2}}} \sum_{k, k_1, k_2 \in \Omega} e^{-i\phi_{k_1} r - i\phi_{k_2} s + i\phi_k n} \langle b_{k_1}^\dagger b_{k_2}^\dagger b_k b_q \rangle. \quad (\text{D.11})$$

Applying the Wick's theorem, we get

$$\begin{aligned} \langle V_1 | c_r^\dagger c_s^\dagger c_n | J \rangle &= \frac{i}{L^{\frac{3}{2}}} \sum_{k, k_1, k_2 \in \Omega} e^{-i\phi_{k_1} r - i\phi_{k_2} s + i\phi_k n} (\langle b_{k_2}^\dagger b_q \rangle \langle b_{k_1}^\dagger b_k \rangle - \langle b_{k_2}^\dagger b_q \rangle \langle b_{k_1}^\dagger b_k \rangle) \\ &= \frac{i}{L^{\frac{3}{2}}} \sum_{k \in V_1} (e^{-i\phi_k s - i\phi_k(r-n)} - e^{-i\phi_k r - i\phi_k(s-n)}) \\ &= \frac{i}{L} \sum_{k \in V_1} (e^{-i\phi_k(r-n)} g_0(s) - e^{-i\phi_k(s-n)} g_0(r)). \end{aligned} \quad (\text{D.12})$$

The other terms can be obtained in the same way

$$\langle V_1 | c_n^\dagger c_r^\dagger c_s | J \rangle = \frac{i}{L} \sum_{k \in V_1} (e^{-i\phi_k(n-s)} g_0(r) - e^{-i\phi_k(r-s)} g_0(n)). \quad (\text{D.13})$$

$$\langle V_1 | c_n^\dagger c_s^\dagger c_r | J \rangle = \frac{i}{L} \sum_{k \in V_1} (e^{-i\phi_k(s-r)} g_0(n) - e^{-i\phi_k(n-r)} g_0(s)). \quad (\text{D.14})$$

References

- [1] P. Calabrese and J. Cardy, “Entanglement entropy and quantum field theory,” *International Journal of Quantum Information*, vol. 4, 2006.
- [2] J. Eisert, M. Cramer, and M. B. Plenio, “Area laws for the entanglement entropy - a review,” 2008.
- [3] P. Calabrese and J. Cardy, “Entanglement entropy and conformal field theory,” *Journal of Physics A: Mathematical and Theoretical*, 2009.
- [4] N. Laflorencie, “Quantum entanglement in condensed matter systems,” *Phys. Rept.*, vol. 646, pp. 1–59, 2016.
- [5] K. Charles and M. Paul, *Introduction to Solid State Physics*. John Wiley & Sons, 2018.
- [6] J. F. Annett, “Superconductivity, superfluids and condensates,” *Oxford University Press*, 2004.
- [7] M. Goldstein and E. Sela, “Symmetry-resolved entanglement in many-body systems,” *American Physical Society*, no. 20, 2018.
- [8] E. Cornfeld, M. Goldstein, and E. Sela, “Imbalance entanglement: Symmetry decomposition of negativity,” *Phys. Rev. A*, vol. 98, no. 3, p. 032302, 2018.
- [9] H.-H. Chen, “Symmetry decomposition of relative entropies in conformal field theory,” *JHEP*, vol. 07, p. 084, 2021.
- [10] R. Bonsignori, P. Ruggiero, and P. Calabrese, “Symmetry resolved entanglement in free fermionic systems,” *J. Phys. A*, vol. 52, no. 47, p. 475302, 2019.
- [11] S. Murciano, G. Di Giulio, and P. Calabrese, “Symmetry resolved entanglement in gapped integrable systems: a corner transfer matrix approach,” *SciPost Phys.*, vol. 8, p. 046, 2020.
- [12] H.-H. Chen, “Charged Rényi negativity of massless free bosons,” *JHEP*, vol. 02, p. 117, 2022.
- [13] D. X. Horváth and P. Calabrese, “Symmetry resolved entanglement in integrable field theories via form factor bootstrap,” *JHEP*, vol. 11, p. 131, 2020.
- [14] S. Fraenkel and M. Goldstein, “Symmetry resolved entanglement: Exact results in 1D and beyond,” *J. Stat. Mech.*, vol. 2003, no. 3, p. 033106, 2020.
- [15] S. Murciano, G. Di Giulio, and P. Calabrese, “Entanglement and symmetry resolution in two dimensional free quantum field theories,” *JHEP*, vol. 08, p. 073, 2020.
- [16] D. Azses and E. Sela, “Symmetry-resolved entanglement in symmetry-protected topological phases,” *Phys. Rev. B*, vol. 102, no. 23, p. 235157, 2020.
- [17] G. Perez, R. Bonsignori, and P. Calabrese, “Quasiparticle dynamics of symmetry-resolved entanglement after a quench: Examples of conformal field theories and free fermions,” *Phys. Rev. B*, vol. 103, no. 4, p. L041104, 2021.
- [18] H.-H. Chen, “Dynamics of charge imbalance resolved negativity after a global quench in free scalar field theory,” *JHEP*, vol. 08, p. 146, 2022. [Erratum: *JHEP* 10, 157 (2022)].
- [19] H.-H. Chen and Z.-X. Huang, “Dynamics of charge imbalance resolved negativity after a local joining quench,” 8 2023.

- [20] A. Rath, V. Vitale, S. Murciano, M. Votto, J. Dubail, R. Kueng, C. Branciard, P. Calabrese, and B. Vermersch, “Entanglement Barrier and its Symmetry Resolution: Theory and Experimental Observation,” *PRX Quantum*, vol. 4, no. 1, p. 010318, 2023.
- [21] B. Bertini, P. Calabrese, M. Collura, K. Klobas, and C. Rylands, “Nonequilibrium Full Counting Statistics and Symmetry-Resolved Entanglement from Space-Time Duality,” *Phys. Rev. Lett.*, vol. 131, no. 14, p. 140401, 2023.
- [22] M. Fossati, F. Ares, and P. Calabrese, “Symmetry-resolved entanglement in critical non-Hermitian systems,” *Phys. Rev. B*, vol. 107, no. 20, p. 205153, 2023.
- [23] A. Lukin, M. Rispoli, R. Schittko, and M. Greiner, “Probing entanglement in a many-body-localized system,” 2018.
- [24] D. Azses, R. Haenel, Y. Naveh, R. Raussendorf, E. Sela, and E. G. Dalla Torre, “Identification of Symmetry-Protected Topological States on Noisy Quantum Computers,” *Phys. Rev. Lett.*, vol. 125, no. 12, p. 120502, 2020.
- [25] A. Neven *et al.*, “Symmetry-resolved entanglement detection using partial transpose moments,” *npj Quantum Inf.*, vol. 7, p. 152, 2021.
- [26] V. Vitale, A. Elben, R. Kueng, A. Neven, J. Carrasco, B. Kraus, P. Zoller, P. Calabrese, B. Vermersch, and M. Dalmonte, “Symmetry-resolved dynamical purification in synthetic quantum matter,” *SciPost Phys.*, vol. 12, no. 3, p. 106, 2022.
- [27] F. Ares, S. Murciano, and P. Calabrese, “Entanglement asymmetry as a probe of symmetry breaking,” 2022.
- [28] L. Capizzi and V. Vitale, “A universal formula for the entanglement asymmetry of matrix product states,” 10 2023.
- [29] F. Ares, S. Murciano, E. Vernier, and P. Calabrese, “Lack of symmetry restoration after a quantum quench: an entanglement asymmetry study,” *SciPost Phys.*, vol. 15, p. 089, 2023.
- [30] B. Bertini, K. Klobas, M. Collura, P. Calabrese, and C. Rylands, “Dynamics of charge fluctuations from asymmetric initial states,” 6 2023.
- [31] L. Capizzi and M. Mazzoni, “Entanglement asymmetry in the ordered phase of many-body systems: the Ising Field Theory,” 7 2023.
- [32] F. Ferro, F. Ares, and P. Calabrese, “Non-equilibrium entanglement asymmetry for discrete groups: the example of the XY spin chain,” 7 2023.
- [33] C. Rylands, K. Klobas, F. Ares, P. Calabrese, S. Murciano, and B. Bertini, “Microscopic origin of the quantum Mpemba effect in integrable systems,” 10 2023.
- [34] S. Murciano, F. Ares, I. Klich, and P. Calabrese, “Entanglement asymmetry and quantum Mpemba effect in the XY spin chain,” 10 2023.
- [35] A. Mollabashi, N. Shiba, T. Takayanagi, K. Tamaoka, and Z. Wei, “Pseudo entropy in free quantum field theories,” 2020.
- [36] A. Mollabashi, N. Shiba, T. Takayanagi, K. Tamaoka, and Z. Wei, “Aspects of pseudo entropy in field theories,” 2021.
- [37] S. Murciano, P. Calabrese, and R. M. Konik, “Generalized entanglement entropies in two-dimensional conformal field theory,” *JHEP*, vol. 05, p. 152, 2022.

- [38] Z. Ma, C. Han, Y. Meir, and E. Sela, “Symmetric inseparability and number entanglement in charge-conserving mixed states,” *Phys. Rev. A*, vol. 105, no. 4, p. 042416, 2022.
- [39] C. Han, Y. Meir, and E. Sela, “Realistic Protocol to Measure Entanglement at Finite Temperatures,” *Phys. Rev. Lett.*, vol. 130, no. 13, p. 136201, 2023.
- [40] F. C. Alcaraz, M. I. Berganza, and G. Sierra, “Entanglement of low-energy excitations in Conformal Field Theory,” *Phys. Rev. Lett.*, vol. 106, p. 201601, 2011.
- [41] M. I. Berganza, F. C. Alcaraz, and G. Sierra, “Entanglement of excited states in critical spin chains,” *J. Stat. Mech.*, vol. 1201, p. P01016, 2012.
- [42] L. Capizzi, P. Ruggiero, and P. Calabrese, “Symmetry resolved entanglement entropy of excited states in a CFT,” *J. Stat. Mech.*, vol. 2007, p. 073101, 2020.
- [43] P. Di Francesco, P. Mathieu, and D. Senechal, *Conformal Field Theory*. Graduate Texts in Contemporary Physics, New York: Springer-Verlag, 1997.
- [44] M.-C. Chung and I. Peschel, “Density-matrix spectra of solvable fermionic systems,” *Phys. Rev. B*, vol. 64, p. 064412, 2001.
- [45] I. Peschel, “Calculation of reduced density matrices from correlation functions,” 2002.
- [46] I. Peschel and V. Eisler, “Reduced density matrices and entanglement entropy in free lattice models,” *Journal of Physics A Mathematical General*, vol. 42, no. 50, pp. 872–893, 2009.
- [47] R. Podgornik, “Book review: Quantum phase transitions. s. sachdev, cambridge university press, 1999,” *Journal of Statistical Physics*, vol. 103, no. 5, pp. 1139–1141, 2001.
- [48] M. Fagotti and P. Calabrese, “Entanglement entropy of two disjoint blocks in xy chains,” *Journal of Statistical Mechanics: Theory and Experiment*, 2010.
- [49] S. Sachdev, *Quantum Phase Transitions*. Handbook of Magnetism and Advanced Magnetic Materials, 2011.
- [50] G. Vidal, J. I. Latorre, E. Rico, and A. Kitaev, “Entanglement in quantum critical phenomena,” *Phys. Rev. Lett.*, vol. 90, p. 227902, 2003.
- [51] R. Balian and E. Brezin, “Nonunitary bogoliubov transformations and extension of wick’s theorem,” *Il Nuovo Cimento B*, vol. 64, no. 1, pp. 37–55, 1969.